

ICEMG 2023-XXXXX

Fast Dynamic Dynamometer System for Testing Variable Speed Drive Under Non-linear Mechanical Loads

Hossein Azizi Moghaddam¹, Arman Farhadi²

¹Niroo Research Institute, Tehran; hmoghaddam@nri.ac.ir

¹Niroo Research Institute, Tehran; afarhadi@nri.ac.ir

Abstract

The evaluation and laboratory study of the electrical machines and their drive system can guarantee an optimum design and utilization of electrical drives in many industrial and research-based applications. Therefore, the testing standards and their required equipment are provided from the beginning of electrical motors commercialization. Using a mechanical load emulator is mandatory for performing programmable tests with the lowest cost and the highest accuracy. In recent years, the producers of electrical machine test benches have introduced the utilization of AC dynamometers as the new generation of these types of equipment. The emulation of the transient behaviors and the load torque complex dynamics entails a fast dynamic drive system to follow the high-frequency reference torque signals with high precision. The proposed dynamometer, as instrumentation equipment, is capable of providing a wide-band torque response in the transient and steady state for the machine under test. The wide-band dynamic response of the proposed dynamometer for emulating several linear and non-linear loads is validated by simulations and experimental results.

Keywords: wide-band dynamometer, dynamic load emulation, nonlinear loads

Introduction

The dynamometer is a practical device for testing electrical machines. It provides a programmable torque to emulate various mechanical load characteristics for the machine under test. The mechanical load characteristics include the static torque component, dynamic torque component, and the mechanical load's non-linear components. In recent decades, various dynamometers have been introduced in the market with different limitations. The dynamometers such as eddy current, magnetic powder, hysteresis, and hydraulic are used only for testing the motors in the first and third regions. Furthermore, these dynamometers are only appropriate for the emulation of static torque components with no application for dynamic torque components. The dynamometer of reference [1] has the ability of dynamic torque emulation, but it uses a DC motor for the emulation. Due to the low speed dynamic response compared with the AC motors, DC motors are inappropriate for the new generation dynamometers. The new generation of AC dynamometers has considerable advantages compared with the typical older types. In addition to the capability for regenerating the brake power to the network, the AC dynamometers are able to emulate the dynamic characteristics of non-linear and

complex mechanical loads due to their fast dynamic response. In reference [2], only linear loads are emulated by the AC dynamometer, and the non-linear loads are not emulated. The dynamometers of [3]-[8] emulated only one type of non-linear load and did not consider other linear and non-linear loads. In references [9]-[11], the AC dynamometer emulated different non-linear loads. However, some of these loads are not common in industrial drives and are just hypothetical non-linear loads.

In traditional classifications, the load torque of electrical drive systems is categorized into six groups constant, frictional, quadratic, constant power, path-dependent, and rotor angle-dependent [12]. Various non-linear loads of the electrical drive systems are classified in [13]. As a dynamometer is an instrumentation equipment, the driver system must provide high precision and fast dynamic response for the torque in the transient and the steady state. After evaluating the dynamometer drive system performance in the torque and speed control modes, the torque control method is selected due to its fast dynamic and wide-band response.

The simulation and experimental results of the proposed AC dynamometer with the capability of emulating various types of non-linear loads with different bandwidths are presented in this paper. The obtained results will show the capability of the implemented dynamometer system for loading the static and dynamic characteristics. The possibility of loading complex mechanical loads, such as misalignment and crankshaft loads, is one of the advantages of the implemented dynamometer system. In addition to the implementation of the hardware sections, a software environment is also provided for performing different test scenarios settings, device protection, data acquisition, data processing, and data extraction. Therefore, the specifications of the proposed dynamometer can be expressed as follows:

- The capability of testing the motor in the four regions of the speed-torque characteristic.
- The capability of emulating the load torque static and dynamic components.
- High flexibility in the implementation of different scenarios and the combination of various load characteristics.
- The capability of emulating the non-linear components and industrial complex loads.

The Control Approach of Proposed Dynamometer

The dynamometer consists of three building parts including an electrical machine as a dynamometer, power electronic converters, and measuring sensors. Figure 1 shows the control approach of the dynamometer, which is based vector method. In this method, the motor speed ω_r ,

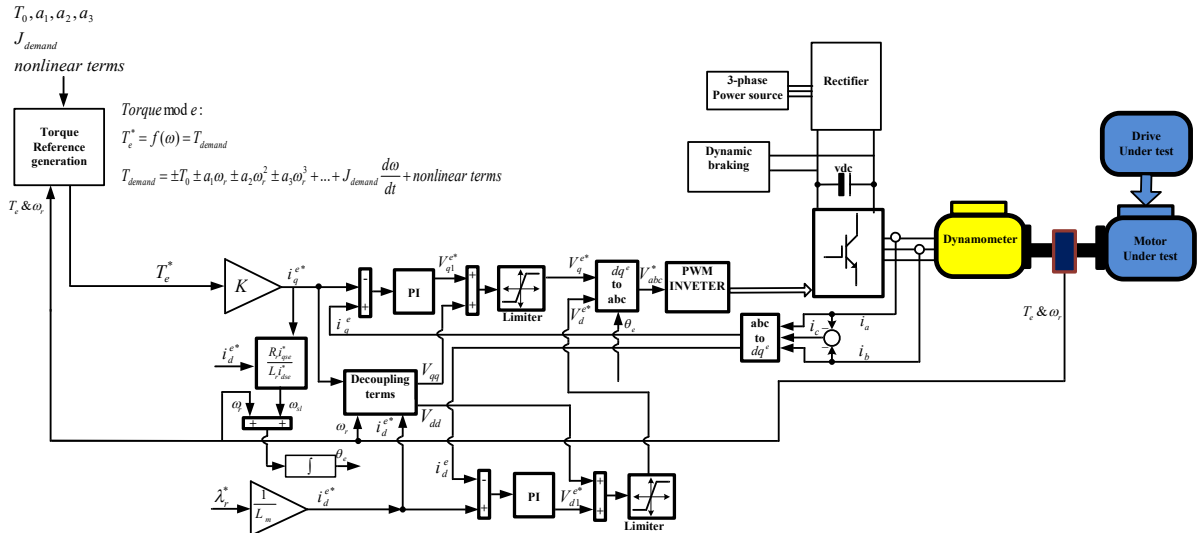


Figure 1. Block diagram of dynamometer control according to FOC method

is measured, and the instantaneous value of the torque, based on the analytical relation between the torque and speed, is calculated and applied to the dynamometer's driver system as the reference torque T_e^* . The dynamometer drive system must track the desired reference torque. The reference torque value, from an exterior loop, is calculated based on (1) and applied to the FOC controller, as shown in Figure 2. The inverter voltage reference V^{*abc} is obtained after reference currents calculation along the two axes dq using the current controllers. Finally, the modulator provides the inverter switching PWM pulses based on the calculated reference voltages. In this approach, the measured motor speed ω_r is applied to the coupling model to obtain the speed ω_r' . The coupling model can emulate the coupling system's non-linear effects. In the case of neglecting the coupling model, then ω_r will be equal ω_r' .

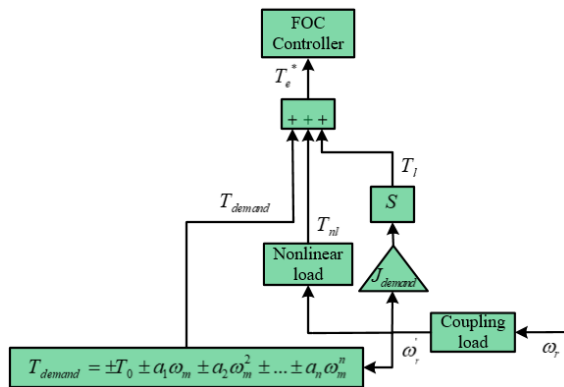


Figure 2. Block diagram of torque reference generation

Considering the effects of linear and non-linear loads, the reference torque T_e^* of the FOC method is calculated as:

$$T_e^* = f(\omega_r) = T_{demand} \quad (1)$$

$$T_{demand} = \pm T_0 \pm a_1 \omega_r \pm a_2 \omega_r^2 \pm a_3 \omega_r^3 \pm \dots \pm J_{demand} \frac{d\omega_r}{dt} + T_{nl}$$

where, T_{demand} is the requested load torque, T_{nl} is the non-linear torque of the load, T_0 is the constant torque component of the load, a_1, a_2, \dots is the coefficient of the

load torque function, and J_{demand} is the requested inertia of the load.

Therefore, by defining parameters: $T_0, a_1, a_2, \dots, J_{demand}$ and T_{nl} , the reference torque value T_e^* is calculated in terms of the speed of the axis between the motor and dynamometer and is applied to the vector control method.

Simulation results

This section discusses the simulation of several non-linear loads by the AC dynamometer. The torque control method, as shown in figure 1 and figure 2, is used for controlling the dynamometer. The dynamometer's motor is an induction motor with the parameters defined in Table 1. Also, an induction motor with the parameters of Table 1 is connected to the dynamometer as the motor under test. Figure 3 shows the simulation results of the dynamometer's step response for the nominal torque value of 13 N.m. As can be seen, the dynamometer tracked the reference step well as a result of the system's fast dynamic response. Furthermore, the ability of fast dynamic response allows the dynamometer to emulate the non-linear load torques with the different scenarios.

Table 1. The dynamometer and motor under test parameters

Parameters	Dynamometer motor	Motor under test
Nominal power	4 kw	4 kw
Nominal voltage	380 V	380 V
Nominal speed	2880 rpm	2890 rpm
Pole pairs	1	1
Nominal current	7.6 A	8.17 A
The moment of inertia	0.046 kg/m ²	0.046 kg/m ²

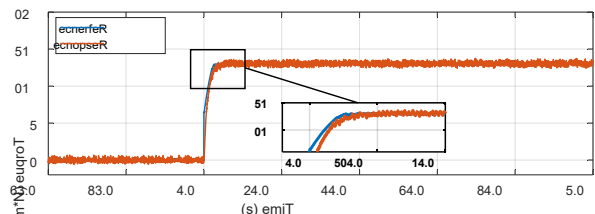


Figure 3. The step response of the dynamometer

In the first scenario, the dynamometer must emulate a sinusoidal load torque with 5 N.m amplitude and a frequency of 40 Hz for the motor under test. The simulation results of this scenario are shown in figure 4. As can be seen, the dynamometer is capable of tracking the sinusoidal reference torque with a fast dynamic response. Therefore, the dynamometer can emulate any load torque with high-frequency non-linear components.

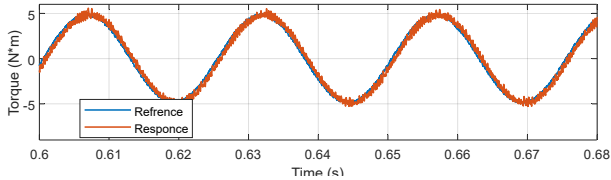


Figure 4. The dynamic response for 40 Hz sinusoidal torque

In the second scenario, the dynamometer must simulate the misalignment load torque. Figure 5 shows the misalignment load model. In the misalignment load model, the motor under the test shaft is connected to the load with the angle β , which causes unwanted sinusoidal torques in the system.

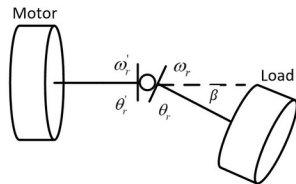


Figure 5. The model of misalignment load

The reference [14] provides a more detailed analysis of misalignment load torque relationships. Since misalignment load torque is of the coupling type, it converts the measured speed of the motor ω_r to the coupling speed ω_r' by the following relation:

$$\omega_r' = \frac{\cos(\beta)}{1 - \sin^2(\beta)\cos^2(\theta_r)} \omega_r \quad (2)$$

where the angular position of the load motor can be denoted as $\theta_r = \omega_r t$.

Figure 6 shows the result of the misalignment load torque simulation for the dynamometer. Here, the angle $\beta=5^\circ$ is considered. The simulation scenario is that at the moment s 0.6, the system speed has increased from 2500 rpm to 2900 rpm. The dynamometer emulates misalignment load torque accurately at 2500 rpm and 2900 rpm steady state speeds.

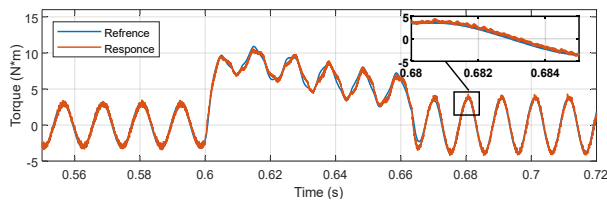


Figure 6. Misalignment load simulation results

In the third scenario, the crankshaft load torque, which has a more complex non-linear behavior, is investigated. Figure 7 shows the model of the crankshaft mechanical load. Compressors, equipped with drive

systems, are one of the loads that indicate the crankshaft mechanism.

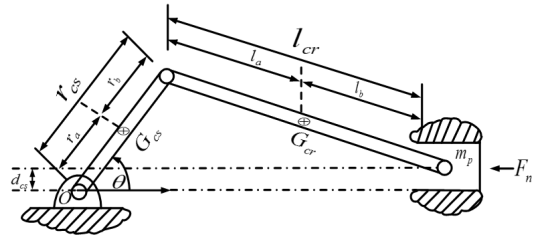


Figure 7. The model of crankshaft load

In the crankshaft mechanism, the relation between the load's torque with the speed, position, inertia, and other geometrical parameters are modeled as follows:

$$T_{nl} = (J_m + J_{cs}(\theta_r)) \frac{d\omega_r}{dt} + F_n r_{cs} \left(\sin(\theta_r) + \frac{\frac{r_{cs}}{l_{cr}} \sin(2\theta_r)}{\sqrt{1 - \left(\frac{r_{cs}}{l_{cr}} \sin(\theta_r)\right)^2}} \right) \quad (3)$$

where J_m , F_n , l_{cr} , and r_{cs} are the motor moment of inertia, the normal force, the connecting rod length, and the crank length, respectively. The term $J_{cs}(\theta_r)$ is the inertia moment of the crankshaft mechanism, which is not considered here for simplicity [15].

Figure 8 shows the simulation result of the crankshaft load. The simulation scenario is such that at the beginning, the reference speed of the motor is 1000 rpm, and at the instant of 0.6 s, the speed has increased to 2300 rpm. At 1000 rpm and 2300 rpm, the dynamometer tracked the torque reference very well.

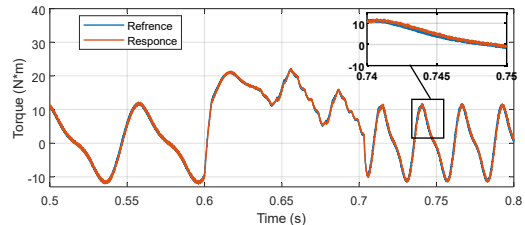


Figure 8. Crankshaft load simulation results

Experimental results for linear loads

In this section, some linear loads are emulated by the proposed dynamometer. Figure 9 shows the experimental implementation of the dynamometer system. The controlling algorithm is programmed on a DSP TMS320f335 processor. The motor under test is controlled using EURO THERM drive AC690. The drive of the motor under test is based on the V/F method. The dynamometer motor and the motor under test parameters are indicated in Table 1.

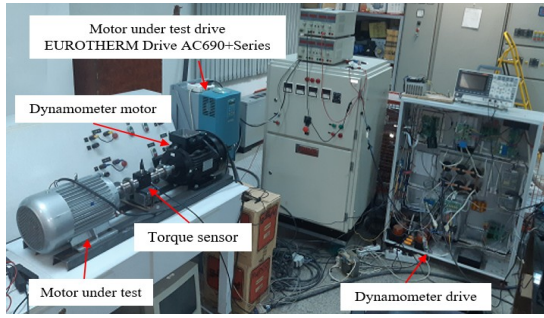


Figure 9. The experiment platform of proposed dynamometer

A. Constant load torque emulation

The system response to the pulse torque reference in the second and third regions of the torque-speed characteristic is investigated in this section. Figure 10 shows the pulse torque reference $T_0 = \pm 3$ N.m (yellow curve), the dynamometer motor torque (blue curve), and the stator current. As can be seen, the dynamometer motor torque tracks the instantaneous reference torque accurately.

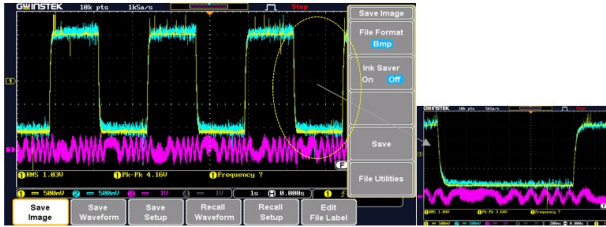


Figure 10. The dynamometer torque response for the pulse torque reference $T_0 = \pm 3$ N.m

B. Programmable constant load torque emulation

Programmable loading of the motor under test based on the user-selected torque profile can be considered one of the advantages of the dynamometer system. Figure 11 shows the motor under test speed (yellow curve), load brake torque (blue curve), and motor stator current (motor under test current) in the condition of applying a step-wise load brake torque from the no-load state to the nominal load state. Therefore, this ability allows an automatic motor testing operation as if when reaching the steady-state condition, the electrical and mechanical quantities are measured, the required data are extracted, and this procedure is repeated for each step of the load torque changes. Finally, by connecting the obtained points, the required characteristic is extracted. In this method, the number of steps and the interval time between applying the torque moments are programmable. Moreover, if the number of steps is increased (for small step sizes), the load torque profile will be a ramp function, where the rate of the slope and the peak of the torque is programmable.

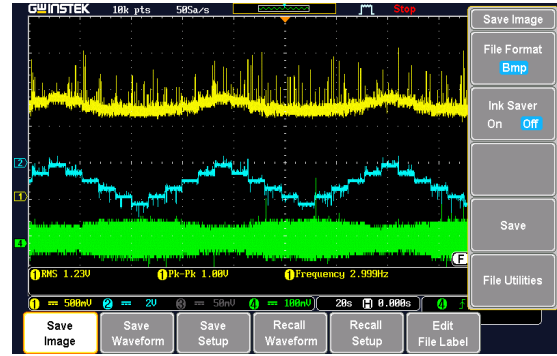


Figure 11. In order from the top: motor under test speed, dynamometer torque, and motor under test current for the programmable load ± 12 N.m

C. Dynamic load torque emulation

The industrial load's torque is composed of two components of static torque T_{static} and dynamic torque, which is represented as follows:

$$T_l = T_{static} + J_{load} \frac{d\omega_r}{dt} \quad (4)$$

Here J_{load} and T_l are load inertia momentum and the load reference torque, respectively. Programmable loading of the dynamic torque effects resulting from the load inertia is one of the advantages of the proposed dynamometer. This capability of the dynamometer systems is utilized in many laboratory studies of motors and drivers, especially in electrical transportation applications. In this section, the load inertia effects on the dynamometer system-generated torque are tested experimentally. The dynamometer's motor, shown in Figure 12, has inertia $J_{dynamo} = 0.046$ kg/m², which is added to the motor under test inertia. The system's dynamic equation when the motor under test is connected to the dynamometer motor is described as follows:

$$T_M - T_{dynamo} = (J_M + J_{demand} + J_{dynamo}) \frac{d\omega_r}{dt} \quad (5)$$

where J_M , J_{dynamo} , and J_{demand} are the motor under test inertia, the dynamometer's motor inertia, and the required reference inertia for loading on the motor, respectively. The T_M and T_{dynamo} express the motor under test inertia and the dynamometer's motor torque. The J_{demand} inertia value can be more or less than the J_{dynamo} value.

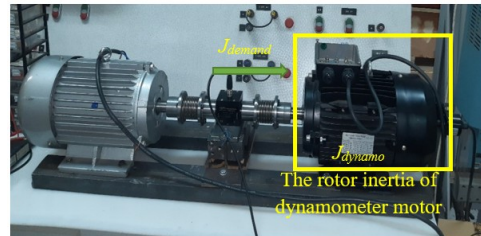


Figure 12. Dynamometer motor and motor under test

Based on equation (4), and considering that the inertia of the dynamometer's motor rotor is imposed on the motor under test, the reference dynamic torque T_l , which has to be generated by the dynamometer's motor, is calculated as:

$$T_l = (J_{demand} - J_{dynamo}) \frac{d\omega_r}{dt} \quad (6)$$

The experimental results for $J_{demand} = 4J_{dynamo}$ are shown in Figure 13. In this condition, the dynamic torque value $3J_{dynamo} \cdot d\omega_r/dt$ is added to the static torque. This dynamic torque term appears in the dynamometer's motor-generated torque from moment A. Decreasing or increasing this torque component is equivalent to decreasing or increasing the load inertia for the motor under test. After the increase of the dynamic torque term by the dynamometer system, the motor's speed dynamic response is made faster under the influence of this dynamic torque term.

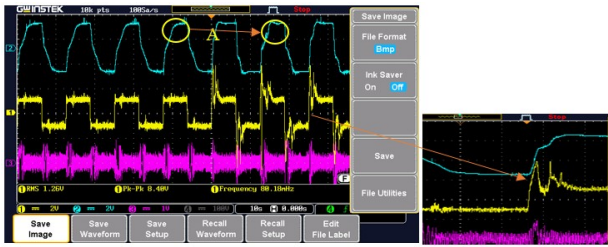


Figure 13. In order from the top: motor under test speed, dynamometer torque, and motor under test current for the inertia $J_{demand} = 4J_{dynamo}$ and the pulse torque reference $T_0 = \pm 3$ N.m

Experimental results for nonlinear loads

In this section, the ability of the proposed dynamometer to emulate two linear loads has been investigated.

A. The determination of dynamometer bandwidth and the ability to generate high-frequency load torque components

The non-linear behavior of the industrial loads and the creation of unwanted high-frequency oscillations in the applied load torque into the motor drive system is unavoidable. These load torque components have typically high-frequency components, and the generation of these mechanical loads high-frequency components in the dynamometer's system needs the utilization of a drive system with a high dynamic response (high bandwidth). To evaluate the performance of the implemented control system for tracking the load torque high-frequency components, the dynamometer's drive system response for the sinusoidal reference torque ± 3 N.m and the frequencies 1Hz to 40Hz is tested. The obtained results from the 1Hz and 40Hz tests are shown in Figure 14 and Figure 15, respectively, where the yellow color represents the reference torque signal, and the blue color expresses the dynamometer's torque. The experimental results show that the implemented drive system is capable of tracking the sinusoidal reference torque up to 40Hz with a fast and high precision dynamic. For the frequencies above 40Hz, the tracking error is increased dramatically, and the increase in the torque ripples causes the improper operation of the dynamometer system. To achieve higher bandwidths, using more complex controlling methods and higher switching frequencies is needed.

B. Misalignment torque emulation

One of the special capabilities of the proposed dynamometer is that the user can change the oscillatory torque parameters resulting from the misalignment load

to observe its effects on the operation of the motor drive system. In the simulation results section, the mathematical relations and misalignment load torque waveforms are investigated. The experimental results for the misalignment load with $\beta = 60^\circ$ is shown in Figure 16. In this scenario, the misalignment load is applied at the moment T1. The experimental results show that, by the increase in the misalignment angle, the load's torque oscillation are increased, where the effects of these high-frequency fluctuations on the motor under test speed can be observed as the oscillations with the same frequency.

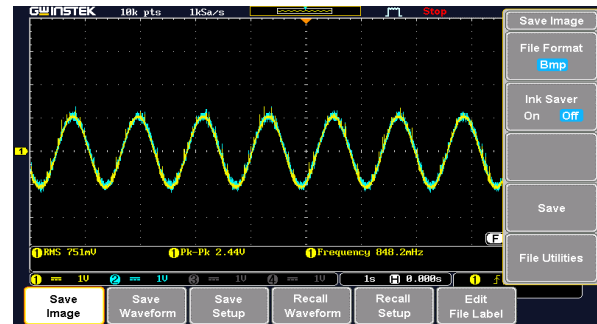


Figure 14. The dynamic response of the dynamometer for 1 Hz sinusoidal reference torque

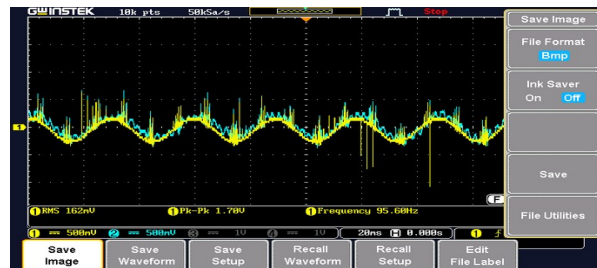


Figure 15. The dynamic response of the dynamometer for 40 Hz sinusoidal reference torque

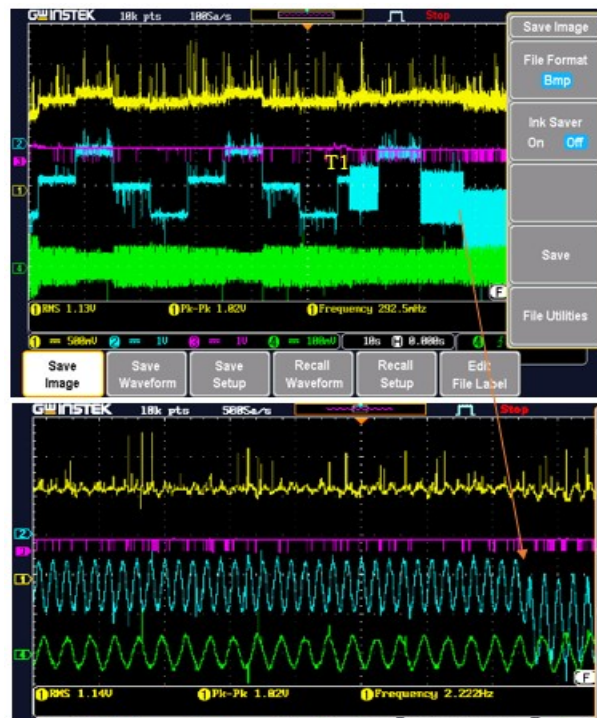


Figure 16. In order from the top: motor under test speed, dynamometer torque, and motor under test current for the misalignment with $\beta=60^\circ$

C. Crankshaft mechanism torque emulation

As discussed in the simulation results, the crankshaft load has a complex behavior, and the dynamometer can emulate that on the motor under test. Figure 17 shows the experimental results for the crankshaft load. In this scenario, the oscillatory component resulting from applying the crankshaft load is applied to the motor under test from the moment T1. As represented in the experimental results (the enlarged section of Figure 17), the dynamometer's torque control system, in addition to the load static torque, generates the oscillatory torque value resulting from the crankshaft load from the moment T1. The effects of oscillatory components of the crankshaft torque on the motor under test speed and the stator current are considerable. Furthermore, Figure 17 shows the dynamometer system behavior in the condition of the changes of the motor under test speed. The crankshaft load torque is dependent on the position and the derivatives of the speed, where the oscillation frequency and its amplitude are affected by the changes in the motor speed, as seen in (3). The effects of these oscillations on the transient speed response and the motor under test steady-state operation are shown in an enlarged view in Figure 17.

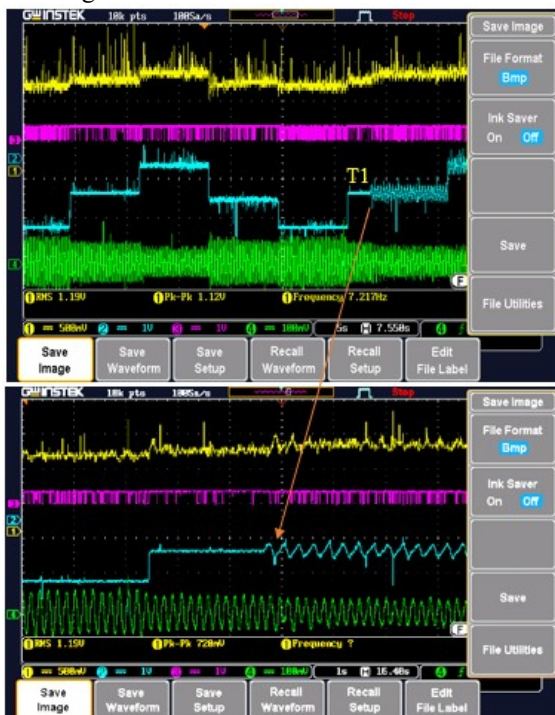


Figure 17. In order from the top: motor under test speed, dynamometer torque, and motor under test current for the crankshaft load

Conclusions

In this paper, different types of static loads, dynamic loads, and high-frequency non-linear components of the typical industrial loads are implemented, and the dynamometer system and the motor under test response are evaluated and analyzed in each case separately. Analysis of the results shows that the implemented

dynamometer is capable of modeling a wide range of industrial load characteristics in the laboratory. The simulation and experimental results revealed that the proposed dynamometer is of a fast dynamic response. This ability can be utilized efficiently for the emulation of the non-linear components in the frequency range of 1Hz to 40Hz, which is present in the misalignment or crankshaft loads. Using the proposed dynamometer system, the user can utilize programmable loading of diverse combinations of the different industrial load's components (static, dynamic, and non-linear components) on the motor under test and analysis the motor drive system under test.

References

- [1] C. R. Hewson, M. Sumner, G. M. Asher, and P. W. Wheeler, 2000. "Dynamic mechanical load emulation test facility to evaluate the performance of AC inverters". *Power Engineering Journal*, 14(1), Feb., pp. 21-28.
- [2] K. Kyslan and F. Durovsky, 2013. "Dynamic Emulation of Mechanical Load – An Approach Based on Industrial Drives Features". *Automatika*, 54(3), Sept., pp. 356–363.
- [3] M. Rodic, K. Jezernik, and M. Trlep, 2006. "Dynamic emulation of mechanical loads: an advanced approach". *IEE Proceedings - Electric Power Applications*, 153(2), March, pp. 159-166.
- [4] J. Arellano-Padilla, G. M. Asher, and M. Sumner, 2006. "Control of an AC Dynamometer for Dynamic Emulation of Mechanical Loads With Stiff and Flexible Shafts". *IEEE Transactions on Industrial Electronics*, 53(4), June, pp. 1250-1260.
- [5] S. K. Bagh, P. Samuel, R. Sharma, and S. Banerjee, 2012. "Emulation of Static and Dynamic Characteristics of a Wind Turbine using Matlab/Simulink". *2nd Inter. Conf. Power, Control and Embedded Systems*, Dec., pp. 159–166.
- [6] C. Gan, R. Todd, and J. M. Apsley, 2015. "Drive System Dynamics Compensator for a Mechanical System Emulator". *IEEE Trans. on Industrial Electronics*, 62(1), Jan., pp. 70–78.
- [7] P. Fajri, S. Lee, V. A. K. Prabhala, and M. Ferdowsi, 2016. "Modeling and Integration of Electric Vehicle Regenerative and Friction Braking for Motor/Dynamometer Test Bench Emulation". *IEEE Transactions on Vehicular Technology*, 65(6) June, pp. 4264-4273.
- [8] J. Song-Manguelle, G. Ekemb, D. L. Mon-Nzongo, T. Jin, and M. L. Doumbia, 2018. "A Theoretical Analysis of Pulsating Torque Components in AC Machines With Variable Frequency Drives and Dynamic Mechanical Loads". *IEEE Transactions on Industrial Electronics*, 65(12), Dec., pp. 9311-9324.
- [9] Z. H. Akpolat, G. M. Asher, and J. C. Clare, 1999. "Experimental dynamometer emulation of nonlinear mechanical loads". *IEEE Transactions on Industry Applications*, 35(6), Dec., pp. 1367-1373.
- [10] Z. Hakan Akpolat, G. M. Asher, and J. C. Clare, 1999. "Dynamic emulation of mechanical loads using a vector-controlled induction motor-generator

- set” *IEEE Transactions on Industrial Electronics*, 46(2), April, pp. 370-379.
- [11] C. M. R. de Oliveira, M. L. de Aguiar, A. G. de Castro, P. R. U. Guazzelli, W. C. d. A. Pereira, and J. R. B. d. A. Monteiro, 2020. “High-Accuracy Dynamic Load Emulation Method for Electrical Drives” *IEEE Transactions on Industrial Electronics*, 67(9), Sept., pp. 7239-7249.
- [12] S.K. Pillai, 1990. *A First Course on Electrical Drives*, New Age International, New Delhi.
- [13] H. AziziMoghaddam, A. Farhadi, and S. Mohamadian, 2021. “Non-linearity Effects of Industrial Loads on Induction Motor Servo Drive System”. *Iranian Journal of Electrical and Electronic Engineering*, 18(2), Nov., pp. 2046-2046.
- [14] J. M. Bossio, G. R. Bossio, and C. H. De Angelo, 2009. “Angular misalignment in induction motors with flexible coupling”. *35th Annual Conference of IEEE Industrial Electronics*, Nov., pp. 1033-1038.
- [15] B. Chen, Y. Wu, and F. Hsieh, 2010. “Estimation of Engine Rotational Dynamics Using Kalman Filter Based on a Kinematic Model”. *IEEE Transactions on Vehicular Technology*, 59(8), Oct., pp. 3728-3735.